A RAPID SEDIMENT ANALYZER FOR SANDS

A RAPID SEDIMENT ANALYZER FOR SANDS

BY

KENNETH DONALD McALPINE

A Thesis

Submitted to the Department of Geology

in Partial Fulfilment of the Requirements

for the Degree

Bachelor of Science

McMaster University

May 1969

BACHELOR OF SCIENCE (1969) McMASTER UNIVERSITY
(Geology) Hamilton, Ontario

TITLE: A rapid sediment analyzer for sands

AUTHOR: Kenneth Donald McAlpine

SUPERVISOR: Professor G. V. Middleton

NUMBER OF PAGES: v, 32

ACKNOWLEDGEMENTS

The writer wishes to express his sincere appreciation to Dr. V. G. Middleton, his supervisor, for his many helpful suggestions and infinite patience.

Thanks are also extended to Dr. J. R. Kramer for his help with the sediment introduction device, and to J. Cekr, who built the apparatus.

Financial support was provided by the National Research Council of Canada.

TABLE OF CONTENTS

LIST OF ILLUSTRATIONS

INTRODUCTION

In recent years considerable research has been undertaken to determine the relationship between sedimentary particles and their dynamic behaviour in the aqueous environment during erosion, transportation and deposition. The gathered data suggests that the terminal fall velocity is an extremely important characteristic of the sediment particles; the fall velocity in turn is a function of the properties of the particles and the surrounding fluid.

For example, Simons and others (1965) concluded from experiments in a recirculating flume that fall velocity is the primary variable that determines the interaction between the bed material and the fluid. Jopling (1965) used the computed settling velocities of sedimentary particles to predict the grain size distributions of the bottomsets and toesets of experimentally produced deltas. He concluded that his "path line method" yielded a reasonable degree of agreement between computed and actual results.

Many problems in the interpretation of ancient and modern sediments are related to settling velocity phenomena. For example, a micaceous sand, composed predominantly of high sphericity quartz grains may contain low sphericity mica flakes of a sieve diameter much larger than the mean sample size and heavy minerals of a much smaller sieve diameter. The difficulty now arises in interpreting whether the deposition of the

mica and heavy mineral fractions occurred under the same sedimentary conditions as the deposition of the quartz or during periods of high and low fluid velocities. As a further extension of this same problem one may consider a suspended load of constant mineralogical composition where differing sphericity values occur. In such a situation there may be an apparent inverse of the general rule that mean particle size decreases in the direction of transportation due to the fact that small, highly spherical particles may settle more quickly than larger low sphericity particles. Plainly, the above problems can only be solved when one studies settling velocities and their relationship to size, shape and density. Thus, a size distribution obtained by settling techniques will be most useful in interpreting the dynamic characteristics of transportation and deposition.

The thesis, then, is to describe a settling tube, built at McMaster University, for the mechanical analysis of sand size samples using settling velocities. This paper outlines the basic theory behind the apparatus, describes the technical data and method of analysis and deduces the accuracy and consistency of the method.

In brief, this sedimentation tube measures the settling velocity distribution of a sediment sample as follows. A pressure transducer consisting of a movable diaphram device continuously measures the pressure differential between two

small outlets in the tube and this data is recorded on a graph electronically. When no sediment is settling in the tube the transducer is essentially measuring the pressure differential between two columns of water with equal heads; that is, zero differential pressure. As soon as sediment is introduced between the two outlets the pressure increases at the lower outlet. Zero differential pressure again occurs in the tube only after all the sediment has settled past the lower outlet. When a range of settling velocities is present in the sample the graphically recorded rate of change of pressure can be calibrated to represent the settling velocity distribution of the sediment. If a size distribution based on any other size parameter such as fall diameter, nominal diameter, sieve diameter, etc. is desired, the settling velocity distribution curve may be analyzed to represent such a size distribution.

THEORY

Mechanical analysis may be defined as the quantitative expression of the size frequency of the particles in a sediment. Because sedimentary particles are not spherical and often highly irregular in shape, size is necessarily poorly defined and may be expressed in a number of ways. Size has variously been expressed as:

1. Volume
2. Weight
3. Surface area
4. Cross sectional area or projection area
5. Settling velocity
6. Intercept through particle or particle projection.

Of these the settling velocity is the fundamental property governing the motion of a sediment particle in a fluid. It is more than merely a measure of physical size, since it is a function of the particle's volume, shape, and density, and the viscosity and density of the fluid.

If an attempt is to be made to use settling velocities as a basis for mechanical analysis of sediments, an understanding of the theory governing the motion of the individual falling particles is required. The theory behind the settling of spherical particles is well known. Excellent summaries may be found in reference number 59-36 of the Woods Hole Oceanographic Institution by Zeigler and Gill (1959) and

report number 12 of the Inter-Agency Committee on Water Resources by Colby and others (1957).

When a particle moves through an extensive, incompressible, viscous fluid at rest two types of forces act over the surface of the particle. Over any infinitesimal area of the particle a pressure force acts normal to that area and a viscous shear force acts parallel or tangentially to the area. The components of these forces taken in the direction of motion of the particle and summed over the entire surface result in what is called profile drag. Moreover, the components of these forces taken normal to the direction of motion and summed over the entire surface result in what is called lift.

The relative importance of the pressure and viscous shear forces, or in other words, the inertia and viscous forces depends on the type of flow situation generated by the particle motion. When a particle is falling slowly or if viscous forces are providing nearly all the resistance to motion, the lines of flow within the fluid are deformed to flow around the particle. In other words the fluid deformation is sufficiently gradual that flow lines do not become unstable and the flow remains laminar. At thigher fall velocities viscous forces are reduced, inertia forces increase in magnitude and the flow becomes turbulent.

Basically, these forces acting on a settling particle can be described in terms of three parameters:

1. Reynolds number
2. a drag coefficient
3. an expression of shape.

The Reynolds number,

$$Re = \frac{vd_n}{\nu}$$

where v = settling velocity of a particle

d_n = nominal diameter: diameter of a sphere having the same volume as the particle

ν = kinematic viscosity of the fluid

is a dimensionless ratio which describes the relative importance of the inertia and viscous forces in determining the fall velocity. Large Reynolds numbers indicate large inertia forces compared to viscous forces, a condition which results in turbulent flow. On the other hand, small Reynolds numbers indicate relatively small inertia forces and are associated with laminor or viscous flow.

The drag coefficient,

$$C_D = \frac{4\ d_n(\rho_s-\rho_f)g}{3\ \rho_f v^2}$$

where: ρ_s = density of the particle

ρ_f = density of the fluid

g = acceleration due to gravity

is a dimensionless ratio which measures the retarding force acting on the falling particle. This retarding force is caused

by profile drag and lift, which in turn, are a result of the pressure and viscous shear forces.

Under conditions of laminar flow, or in general when the Reynolds number is less than 0.1, viscous shear forces account for most of the drag. As the Reynolds number or fall velocity increases the flow gradually becomes turbulent and the drag is better described by pressure or inertia forces. Turbulences begin at Reynolds numbers of about 3 and become well formed at Reynolds numbers of about 3 and become well formed at Reynolds numbers of about 20.

The shape of the falling particle largely determines the path that the flow lines take around it. When the flow is laminar the flow lines merely move around the corners and edges of irregular particles without become unstable. Therefore, during laminar flow the shape is not a very important parameter in determining the fall velocity. At higher fall velocities shape is the major factor controlling the form and intensity of the turbulence and, thus, must be taken into account in computing the fall velocity.

Since sedimentary particles possess an infinite variety of shapes it is impossible to define completely an expression for shape. Of the many shape factors which have been suggested the most satisfactory one appears to be:

$$S.F. = c/\sqrt{ab} \qquad \text{(McNown and Malaika, 1950)}$$

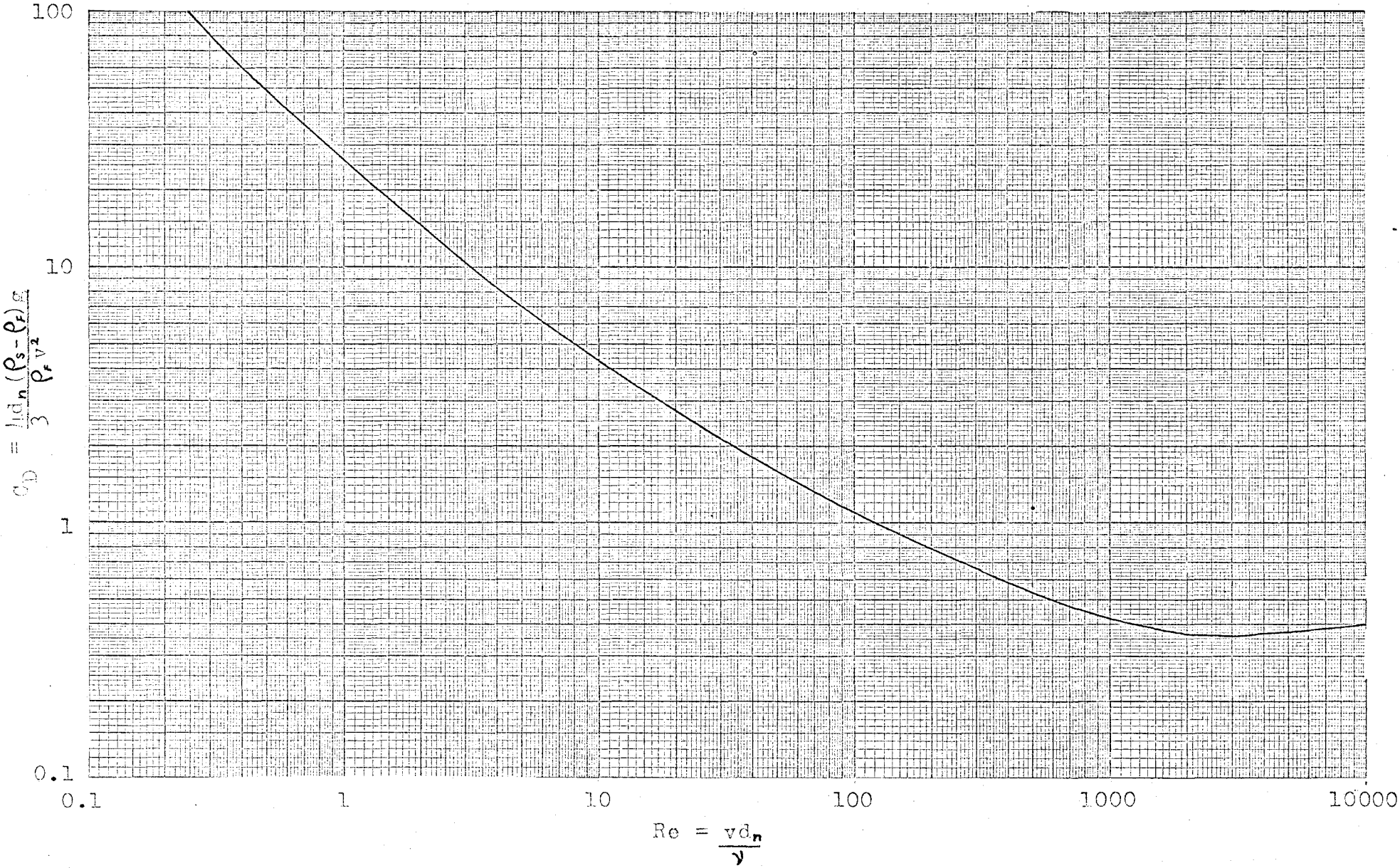

FIG. 1- C_D vs R_e RELATIONSHIP FOR SPHERES

where; a = longest axis

b = intermediate axis

c = shortest axis of the three mutually perpendicular axes of the particle.

From the theoretical discussion of Re and C_D it appears that:

$$C_D = f(Re) \ .$$

In fact, a dimensionless C_D-Re diagram shows that for any particular shape the drag coefficient is a function of the Reynolds number up to very high values (Re = 500,000 for spheres). C_D-Re diagrams have been determined empirically for various shape factors including spheres. In graphs such as figure 1 there are six variables involved in the computations. If any one variable is unknown, sya fall velocity, it can be found by trial and error solution of the C_D and Re equations using the corresponding curve (Colby and others, 1967).

In the preceding discussion a procedure has been described whereby the fall velocity of individual grains settling in an extensive fluid may be calculated. In a settling tube, where there is a population of grains present and the sides of the tube are restricting their fall, errors arise due to the mass properties of the sediment. These errors may be grouped under:

1. Hindered settling
2. Wall interference

3. Settling convection (Kuenen, 1968).

Hindered settling, which results from the mutual interference of settling particles, is related to the concentration of the sample, and wall interference effects are related to the size of the settling tube (Vanoni and others, 1962) (Colby and others, 1957). The combined effects of hindered settling and wall interference are generally thought to be small and quantitative corrections for these errors are generally omitted in settling velocity distribution determinations (Ziegler and others, 1960).

Settling convection signifies the current system set up by differences in density of clouds in a settling suspension (Kuenen, 1968). It tends to increase the fall velocity of sand grains, especially the fine sizes, released at the top of the settling tube. Settling convection is thought to be a much more serious error than hindered settling or wall interference. These errors due to the mass properties of the sediment can be minimized by decreasing the sample size, increasing the diameter of the settling tube and choosing an appropriate method of introduction.

The direct determination of the fall velocity distribution appears to be a logical approach to the classification of sediments, and this can be achieved simply with a sedimentation column. However, the concept of size has been a predominant aspect of sedimentation research for several years.

Therefore, it is mandatory that the fall velocity be related to some measure of "size". The nominal diameter (d_n) of a particle is the diameter of a sphere which has the same volume as the particle. Since volume is a basic measure of size and the fall velocity of a spherical particle can be calculated theoretically, the nominal diameter is generally used to express settling tube values in terms of size.

REVIEW OF PREVIOUS INVESTIGATIONS

Techniques used for the determination of particle size analysis by sedimentation are generally based on two fundamental types of settling systems. A dispersed system is one in which particles of different sizes settle together from an initially uniform dispersion. A system in which particles start settling from a common source is called a stratified system since the falling particles become stratified according to their settling velocities.

In the early 1900's investigations of the analysis of size distribution by sedimentation were mostly based on dispersed systems, whereas later studies tended towards stratified-sedimentation systems which are much moare adaptable to the larger sand sizes. An excellent summary of the early work in this field is given by Krumbein and Pettijohn (1938).

A sedimentation column based on a stratified-sedimination system was developed by Emery (1938). The essential components of Emery's apparatus are a short tube in which the sample is dispersed and a settling column 164 cm. high into the top of which the dispersed sample is poured. Colby and others (1957) developed a visual-accumulation tube which was a modification of the Emery settling tube. Basically they improved the method of introduction of the sample and added a manually operated recording device which provided a permanent and continuous record of accumulation. In both these visual

accumulation methods the volumetric accumulation of deposited sediment with respect to time is measured visually in a contracted section at the bottom of the tube.

Ziegler and others (1960) described the Woods Hole Rapid Sediment Analyzer which automatically records an accumulation curve for a sediment sample. This apparatus measures the difference in hydrostatic pressure generated by sediment in suspension between two points approximately one meter apart by means of a bellows type pressure transducer combined with a chart recorder. In 1966, Schlee modified and calibrated the W.H.R.S.A.

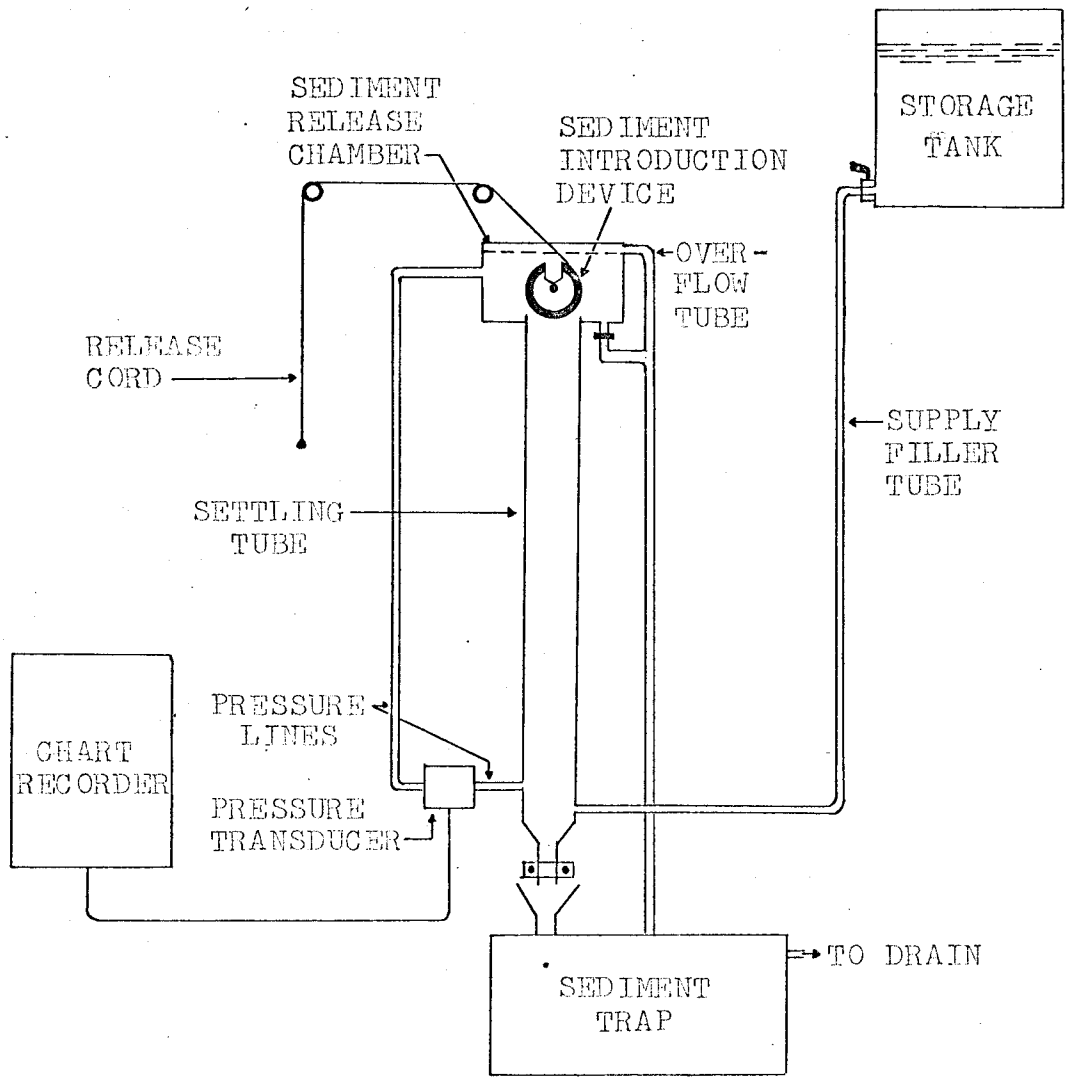

FIG. 2 - SCHEMATIC DIAGRAM OF SETTLING COLUMN SYSTEM

EQUIPMENT

The sediment analyzer (fig. 2 and fig. 3) used in this study is a modification of the original Woods Hole Rapid Sediment Analyzer described by Whitney (1960). The settling tube is 2-1/2 inches inside diameter and 1 metre long from the point of introduction of the sediment to the centreline of the lower pressure tap. Both the settling tube and the sediment release chamber are constructed of lucite plastic. The pressure lines, overflow tube and supply filler tube are rubber.

A storage tank is situated above the level of water in the sediment release chamber and filling of the column is accomplished by gravity feed. An overflow tube is provided to maintain a water level that covers the sediment introduction device and the upper pressure tap. The storage tank holds a supply of distilled water which was equilibrated to the temperature of the entire system. It was found that the distilled water supply available at McMaster University did not require extensive de-aeration as was carried out by Whitney (1960) and Schlee (1966) both of whom used tap water. The distilled water was always allowed to remain in the storage tank at least 24 hours before use, and at no time were bubbles observed to form either in the settling tube or within the pressure sensing system. The sediment release chamber is fitted with a plywood cover to keep out dirt and minimize evaporation.

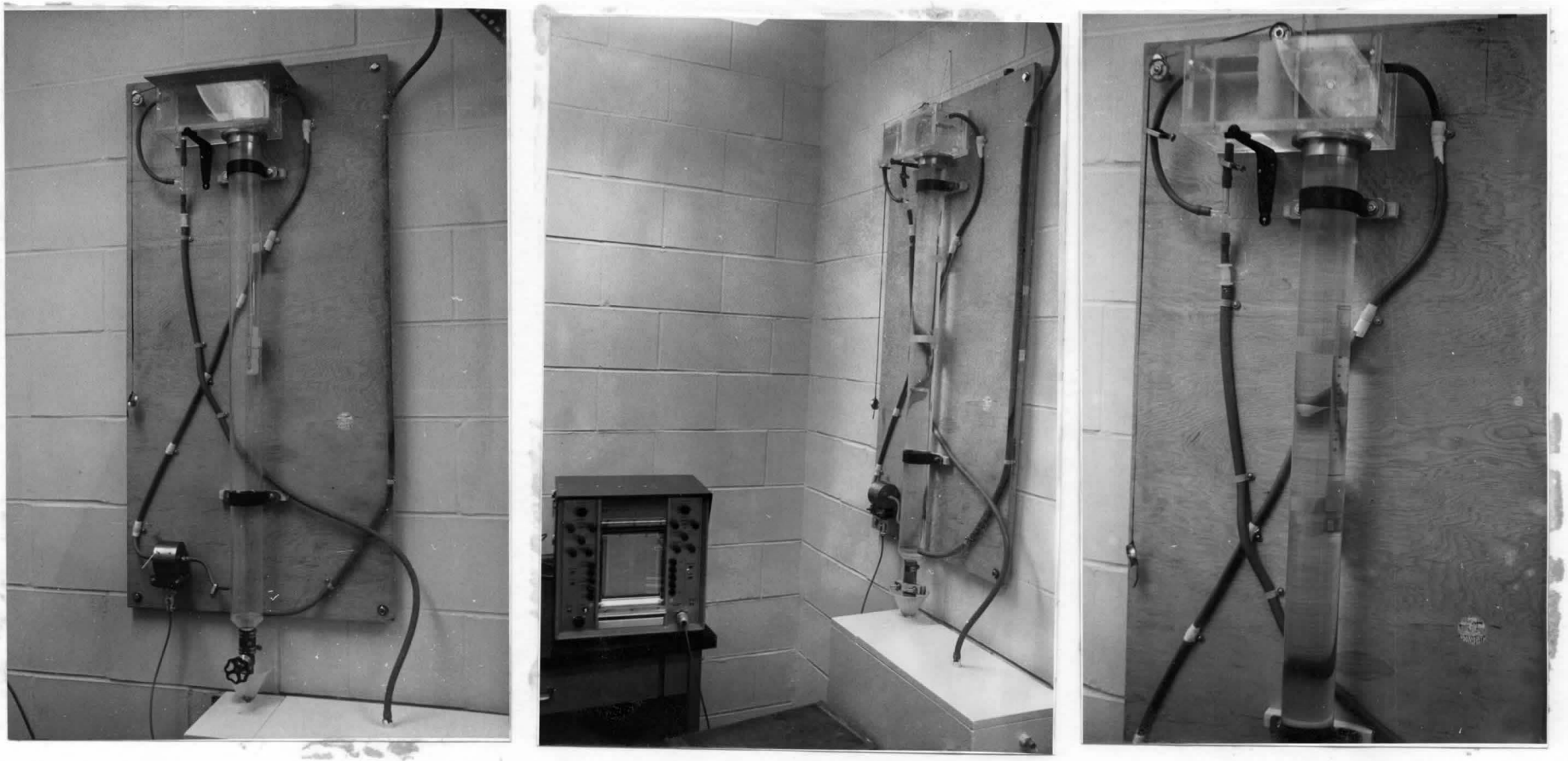

FIG. 3 - McMASTER RAPID SEDIMENT ANALYZER

The main modification of the W.H.R.S.A. was in the construction of the sediment introduction device. Without doubt the method of introduction of a sample into suspension is the most difficult problem to overcome in the design of a settling column. In a column such as the one described here the sample obviously should be introduced at least at the level of the upper pressure tap and preferably between the two pressure taps. Desirable features of a sediment introduction device are:

1. Turbulence eddies and surface wavelets resulting from the settling of the sample itself and from the mechanical action of the release device should be minimized.
2. The sample should begin settling with an initially homogeneous and horizontally dispersed distribution in order to reduce the effects of hindered settling and settling convection.
3. The sample size used should be as small as possible to minimize accelerated settling due to density differences and, at the same time, it should be sufficiently large to be representative of the original population.
4. The sample should be introduced wet.

The device used was suggested by Dr. J. R. Kramer of McMaster University. It consists of a solid lucite plastic cylinder which rotates about a horizontal axis. A hole drilled radially in the cylinder accomodates the sediment sample. The sample is placed in the device with the hole opening upward.

Then the sediment is released into the settling tube when the cylinder is rotated by means of a release cord until the hole opening faces down the tube. Visual observations showed that sediment released in such a manner entered the settling tube uniformly.

The transducer used with the settling tube is a Pace pressure transducer model P90D. The pressure sensing element within the transducer consists of a diaphram placed between two symmetrical core inductance assemblies and separating two pressure chambers. The transducer is equipped with two bleeder valves to eliminate trapped air.

This transducer is coupled with a Sanborn, model 321, amplifier recorder. The recorder provides a chart width of 5 mm., timing marks, several chart speeds, an electric stylus, a pen marker and several attenuator settings.

OPERATIONAL PROCEDURE

Before placing a sample in the analyzer it must be thoroughly wetted and dispersed. Methods of accomplishing these objectives are discussed by Krumbein and Pettijohn (1938) as well as by other standard textbooks of sedimentary petrography. Material beyond the range of sand sizes (coarser than -2.0 Ø and finer than 4.0 Ø) should be screened out (Schlee, 1966). This is especially important if the silt and clay size fraction is large.

In this study the samples were placed in small glass vials which were filled with distilled water and capped at least 24 hours prior to analysis. Dispersion was carried out by vigorous shaking and use of an ultransonic probe in some cases. Each sample was placed in the introduction device by uncapping the vial and holding the thumb over the opening until it was below the water level in the sediment release chamber. After all the sample had been transferred to the introduction device the thumb was replaced over the vial opening and the vial was withdrawn. In this manner several samples could be run without changing the volume of water within the analyzer.

Many test samples showed that the optimum sample sizes were approximately 5 and 10 grams (accurate weighing is not necessary) coupled with attenuator settings on the recorder of 10 and 20 respectively. These values gave the maximum deflection of the pressure curve that would remain on the chart.

Just before a sample is run the sample identification, attenuator setting and water temperature are written on the chart opposite to where the curve is to be recorded. The paper drive is then begun at a speed of 5 mm /sec and the sample is introduced. At the same instant the sample is introduced a stop-watch is started. When the first particle is observed passing the lower pressure tap a time mark is made on the chart. At time 35 seconds of the run the chart speed is changed from 5 mm /sec to 1 mm/sec. Figure 4a shows the record of a run. The purpose of changing the chart speed part way through the run is to increase the slope of the curve and facilitate the reading of data from the curve. After the curve has returned to the baseline the chart drive is turned off and the graph is removed from the recorder for analysis.

The first step in analysis is to mark on the curve the point that corresponds to the time when the first particle passed the lower pressure tap. This point is used to represent the total pressure differential caused by all the sediment in suspension. A size-time overlay (fig. 4b) printed on clear plastic is then used to read the cumulative percent of each size value from the curve. The chart speed changes are incorporated in the overlay and it is placed over the curve so that the 35 second points correspond on both the curve and the overlay. The baseline of the overlay is matched to the projection of the zero differential pressure line of

the curve. Percentiles are found for each point desired using a Gerber variable scale. The Gerber variable scale, which divides a line into 100 equal divisions, is set to the deflection distance (or total pressure point) and then moved along the zero differential pressure line to the size grades (or fall velocities) marked on the overlay.

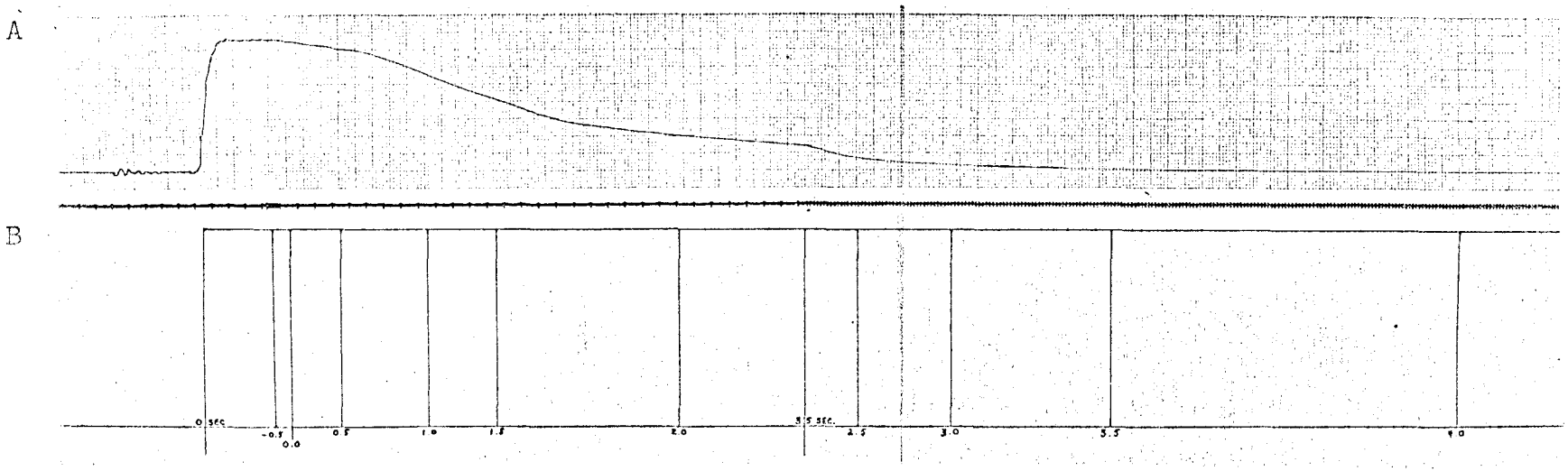

FIG. 4- a. RECORD OF SEDIMENT ANALYSIS. THE INITIAL JUMP AT THE LEFT IS CAUSED BY THE INTRODUCTION OF THE SEDIMENT. THE TICK MARKS AT THE BASE ARE AT ONE SECOND INTERVALS.

b. UNCALIBRATED SIZE-TIME OVERLAY.

EXPERIMENTAL DATA AND ANALYSIS

Standard Samples

The first major obstacle to be overcome in analyzing size by settling velocities is the lack of standard samples with known fall velocity distributions. This is a universal problem in sedimentological research. However, this problem can be overcome. It has been shown previously that the fall velocity for individual spherical particles can be calculated using the well known C_D-R_e relationship. Ideally, quartz spheres could be used to calibrate the settling column directly in terms of the theoretical fall diameter (the diameter of a sphere with a specific gravity of 2.65 and the same fall velocity as the particle).

Since the quartz sphere is a theoretical rather than a practical entity the following procedure was adopted. Glass spheres were obtained commercially and sieved at 1/2 phi intervals. This provided fractions, each with a range of 1/2 phi units, which were recombined to provide samples with known size distributions. Using the C_D-R_e relationship the size distribution was converted to a fall velocity distribution. Because spheres were used, the criticism that fall velocity and sieving measure size in two different ways is not valid in this case.

For determining the fall velocity of an individual particle using the Reynolds number and drag coefficient the nominal diameter of the particle, kinematic viscosity of the

fluid, density of the particle, and the acceleration due to gravity were required.

In this study the nominal diameter was identical to the sieve diameter because spheres were used. No attempt was made to determine the accuracy of the sieves using the optical microscope because the determination of the internal consistency of the experimental data was the prime concern. Moreover, it was believed that if sieve corrections had been made they would have been very small (Colby and others, 1957). Sieve sizes given in this report are, therefore, the nominal values.

All experimental runs were carried out at 22°C. At this temperature the kinematic viscosity and the density of pure water are:

$$\nu = 0.00960 \text{ stokes}$$

$$\rho_f = 0.998 \text{ gm/cm}$$

The density of the glass spheres (ρ_s) was found to vary with size. Calculations with a 5 ml specific gravity bottle gave the following size-density analysis.

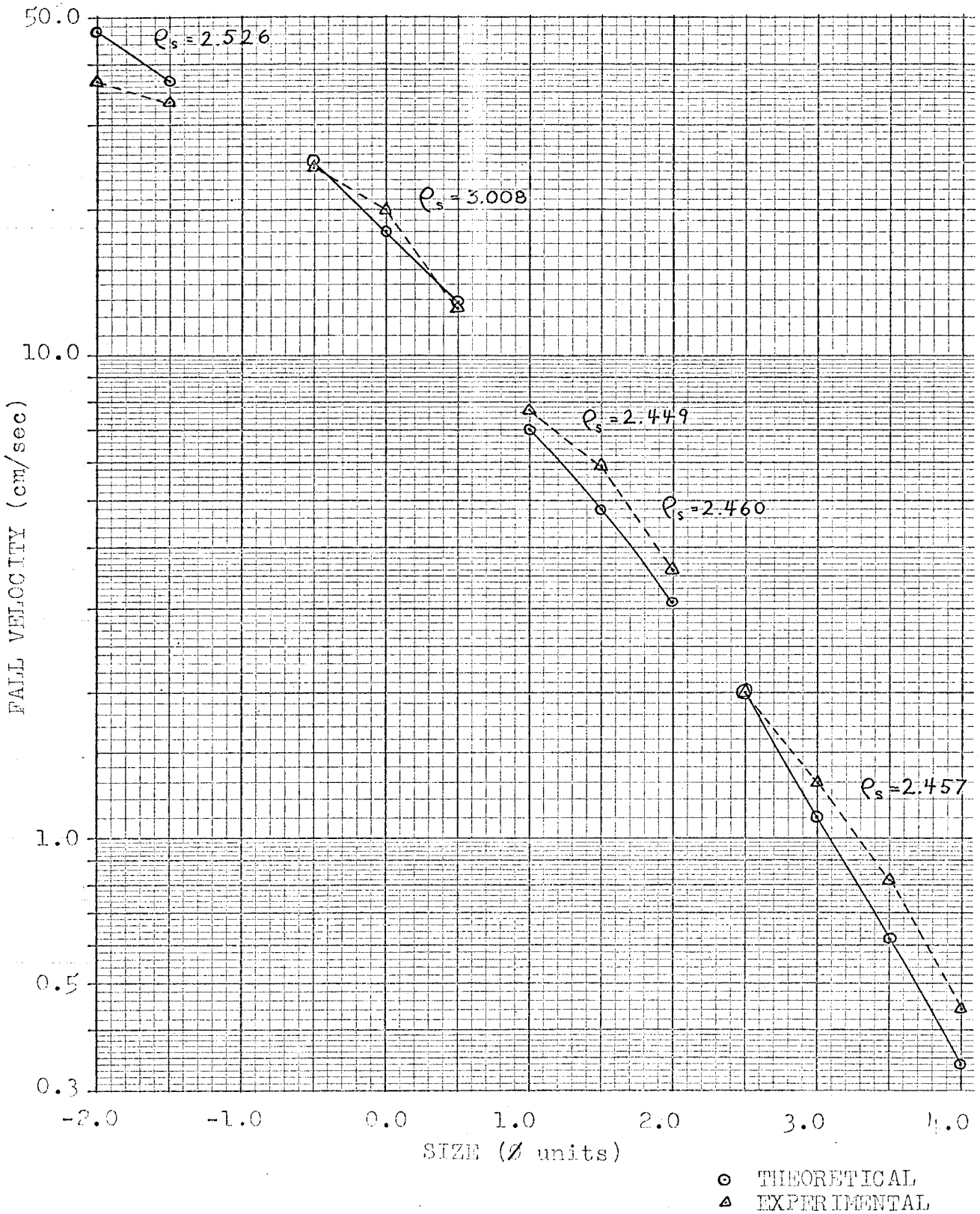

FIG. 5- FALL VELOCITY SIZE GRAPH FOR GLASS SPHERES AT 22°C

TABLE 1

Size* Ø Units	Average fall velocity** $\bar{x}$ - (cm/sec)	σ_x	Theoretical fall velocity*** - (cm/sec)
-2.0	37.0	1.1	47.0
-1.5	33.3	0.0	37.0
-1.0	----	---	----
-0.5	24.4	0.6	24.7
0.0	20.0	0.0	18.0
0.5	12.5	0.0	12.8
1.0	7.7	0.0	7.0
1.5	5.9	0.0	4.8
2.0	3.6	0.1	3.1
2.5	2.0	0.0	2.0
3.0	1.3	0.0	1.1
3.5	0.82	0.0	0.61
4.0	0.44	0.0	0.34

* Determined by seiving
** Calculated experimentally at 22°C
*** Calculated using C_D vs R_e curve at 22°C

Size Ø Units	Density (ρ_s) Run 1	Run 2	Run 3	Average
-0.5 to -2.0	2.528	2.526	2.525	2.526
0.5 to -0.5	3.005	3.010	3.009	3.008
1.5 to 0.5	2.449	2.448	2.451	2.449
2.5 to 1.5	2.454	2.465	2.462	2.460
4.0 to 2.5	2.452	2.458	2.460	2.457

The acceleration due to gravity is 981 cm/sec^2.

Using the above data the theoretical fall velocity was calculated for the 1/2 phi sizes of glass spheres from -2.0 phi to +4.0 phi (table 1 and figure 5). Note that spheres of the -1.0 phi class were not available for the experimental work and, therefore, the fall velocity has not been calculated.

Sensitivity

The first samples run in the sediment analyzer were small charges of glass spheres that were introduced in order to determine the size of the smallest sample that would cause the system to react. The recorder was sensitive to samples as small as 0.01 grams at an attenuator setting of 10. Therefore in a 5 gram sample, the sediment analyzer probably has a sensitivity of 0.2 percent by weight.

Uncalibrated Overlay

Next, sieved fractions of single phi sizes were used to find the experimental fall velocity for each phi class. For each class four samples of 0.5 grams each were run. The

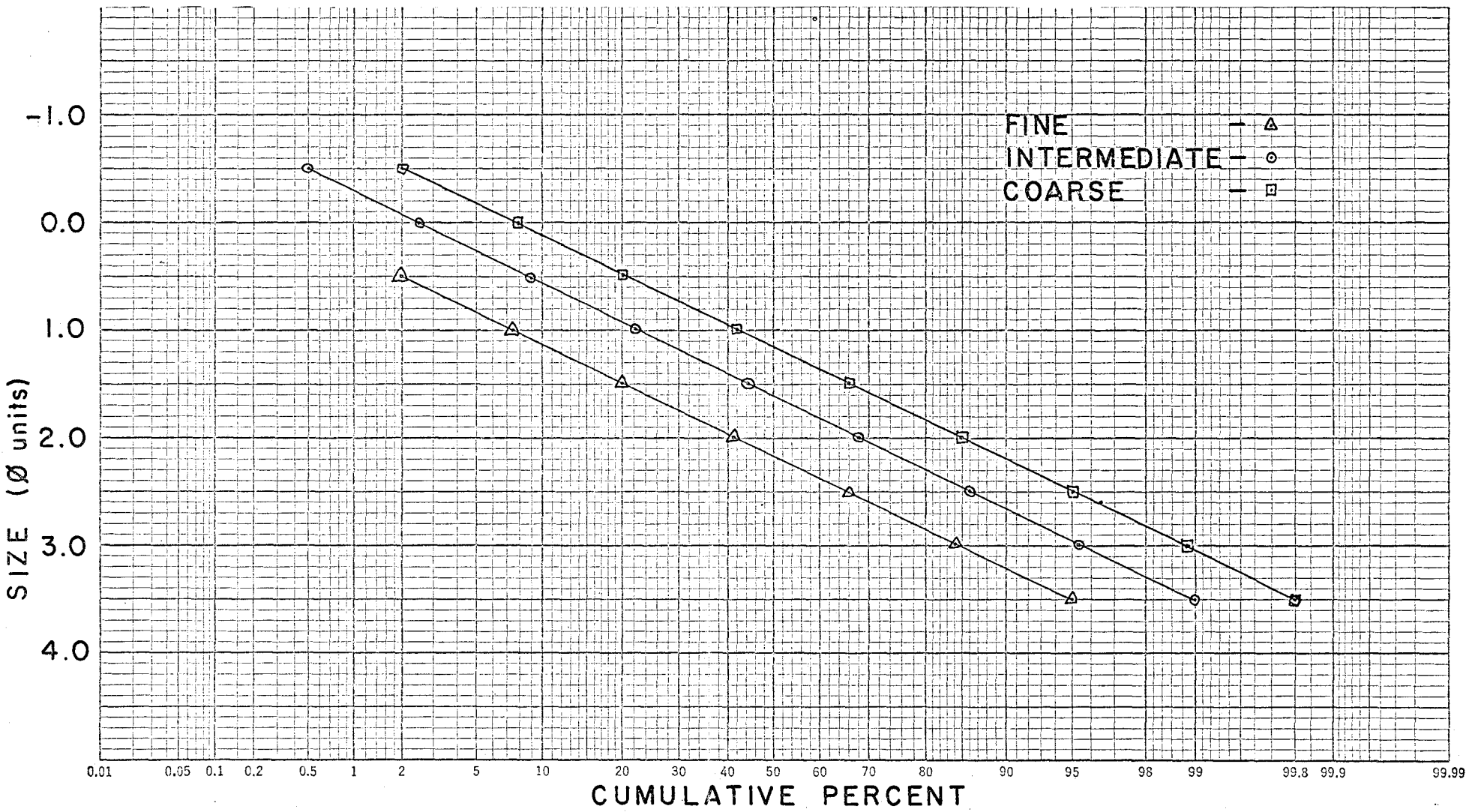

FIG. 6- CUMULATIVE SIZE CURVES FOR THE THREE RECOMBINED GLASS SPHERE SAMPLES

resulting fall velocities for each size were averaged and the standard deviations were calculated. The results are shown in Table 1 and Figure 5. Small samples were used in these runs in order to minimize errors resulting from the mass properties of the sediment.

The fall velocities of the single phi sizes were used to construct an uncalibrated overlay (fig. 4b). The fall times for this overlay were calculated by determining the time it would take for each size of glass spheres to settle 1 metre (the length of the settling tube). This overlay is referred to as uncalibrated because it did not take into account variations in fall time which might result when various size grades are present in a sample distribution.

Consistency

Three artificial sample distributions were then run. A fine, an intermediate and a coarse distribution (fig. 6) were made up to recombining sieved fractions of glass spheres as follows.

Size Ø Units	Distribution -- percent coarser		
	Fine	Intermediate	Coarse
-0.5		0.5	2
0.0		2.5	8
0.5	2	8	22
1.0	7	22	42
1.5	20	44	66
2.0	40	68	85

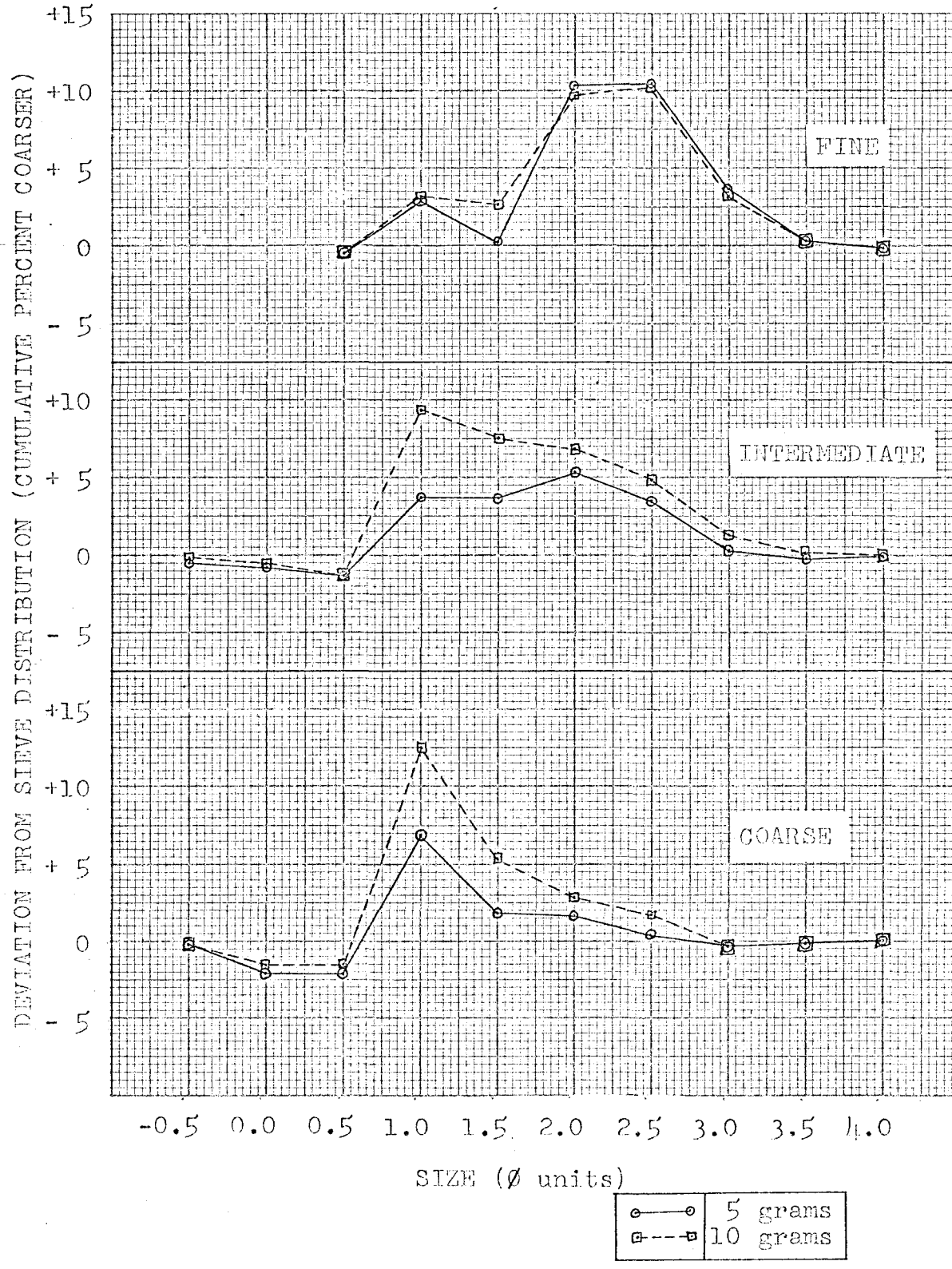

FIG. 7- SIEVE SIZE vs UNCALIBRATED ANALYSIS

2.5	66	86	95
3.0	84	95	98.8
3.5	95	99	99.8
4.0	100	100	100

For each distribution 12 samples of 5 grams each and 12 samples of 10 grams each were run, making a total of 72 runs. Using the uncalibrated overlay the cumulative percent for each phi size in the distribution was read from the recorded pressure curve. The curve analyses are shown in tables 2 and 3. Tables 4 and 5 give the average values for each percentile over the 12 runs and the alculated standard deviations. Figure 7 displays graphically the average deviations of the experimental size distributions from the sieve distributions for each sample.

Analysis of variance tables were calculated for each phi size (0.5 phi to 3.0 phi) in order to determine if the experimental results showed any significant difference between sample sizes (5 and 10 grams) and/or whether there was any significant interaction between the sample sizes and the sample distributions (fine, intermediate and coarse). The results of the analyses of variance are shown in table 6. The total variance for each table is 2 sample sizes × 3 samples × 12 runs.

Significant differences were seen to exist between samples in all cases at the 0.95 level. These were, of course, expected since the samples were made up with different distributions. Significant differences between sample sizes were

observed only for the 1.0 phi class, and significant interaction occurred in the 1.0 phi and 3.0 phi classes.

TABLE 6

For 0.5 Ø

Source of variation	Degrees of Freedom	Sums of Squares	Mean Squares	Variance Ratio	$F_{0.95}$
Between sample sizes	1	0.89	0.89	0.81	3.99
Between samples	2	4486.19	2243.09	2039.17	3.14
Interaction	2	1.19	0.60	0.54	3.14
Error	66	72.60	1.10	—	—
Total	71	4560.88	—	—	—

For 1.0 Ø

Source of variation	Degrees of Freedom	Sums of Squares	Mean Squares	Variance Ratio	$F_{0.95}$
Between sample sizes	1	246.50	264.50	60.80	3.99
Between samples	2	20966.86	10483.43	2409.98	3.14
Interaction	2	121.08	60.54	13.92	3.14
Error	66	287.33	4.35	—	—
Total	71	21639.78	—	—	—

For 1.5 Ø

Source of variation	Degrees of Freedom	Sums of Squares	Mean Squares	Variance Ratio	$F_{0.95}$
Between sample sizes	1	190.13	190.13	2.27	3.99
Between samples	2	28056.25	14028.13	167.44	3.14
Interaction	2	6.58	3.29	0.04	3.14
Error	66	5529.17	83.78	—	—
Total	71	28805.88	—	—	—

(continued)

TABLE 6-(continued)

For 2.0 Ø

Source of variation	Degrees of Freedom	Sums of Squares	Mean Squares	Variance Ratio	$F_{0.95}$
Between sample sizes	1	8.68	8.68	1.56	3.99
Between samples	2	17153.86	8576.93	1539.84	3.14
Interaction	2	18.86	9.43	1.69	3.14
Error	66	367.92	5.57	—	—
Total	71	17549.32	—	—	—

For 2.5 Ø

Source of variation	Degrees of Freedom	Sums of Squares	Mean Squares	Variance Ratio	$F_{0.95}$
Between sample sizes	1	10.89	10.89	3.66	3.99
Between samples	2	4919.69	2459.85	828.23	3.14
Interaction	2	11.19	5.60	1.89	3.14
Error	66	196.16	2.97	—	—
Total	71	5137.94	—	—	—

For 3.0 Ø

Source of variation	Degrees of Freedom	Sums of Squares	Mean Squares	Variance Ratio	$F_{0.95}$
Between sample sizes	1	2.01	2.01	1.84	3.99
Between samples	2	1655.11	827.56	759.23	3.14
Interaction	2	7.00	3.50	3.21	3.14
Error	66	71.83	1.09	—	—
Total	71	1735.95	—	—	—

TABLE 2

Sample- Fine
Size - 5 grams

Size*	Distribution-- percent coarser**											
Ø Units	1	2	3	4	5	6	7	8	9	10	11	12
0.5	1	2	1	0	2	2	1	2	1	2	3	1
1.0	11	12	8	7	11	10	9	9	9	10	14	9
1.5	21	22	18	17	22	18	19	21	18	21	28	17
2.0	58	51	49	49	55	45	51	52	46	52	45	51
2.5	82	81	76	75	77	77	75	72	71	76	80	76
3.0	90	91	86	87	87	88	87	85	85	89	89	88
3.5	98	98	95	95	95	95	95	92	95	95	96	96
4.0	100	100	100	99	100	100	100	99	99	100	100	100

Sample- Intermediate
Size - 5 grams

Size*	Distribution-- percent coarser**											
Ø Units	1	2	3	4	5	6	7	8	9	10	11	12
-0.5	0	0	0	0	0	0	0	0	0	1	0	0
0.0	2	2	2	2	1	1	1	1	2	3	2	1
0.5	7	7	8	7	6	7	4	7	7	8	7	4
1.0	22	25	26	29	24	24	25	28	23	30	28	23
1.5	45	47	46	50	47	46	45	50	51	50	47	47
2.0	74	70	73	73	74	74	72	76	74	72	73	74
2.5	90	89	90	91	90	90	87	91	89	90	90	87
3.0	96	95	96	95	96	95	95	96	95	95	95	94
3.5	99	99	99	99	99	98	99	99	98	99	99	98
4.0	100	100	100	100	100	99	100	100	100	100	100	100

(continued)

TABLE 2-(continued)

Sample- Coarse
Size - 5 grams

Size*	Distribution--percent coarser**											
Ø Units	1	2	3	4	5	6	7	8	9	10	11	12
-0.5	3	1	1	1	2	2	4	3	1	1	1	1
0.0	7	5	7	6	5	8	7	7	5	5	4	5
0.5	20	20	20	20	20	21	21	22	19	18	19	19
1.0	50	50	48	49	50	49	49	51	48	46	50	47
1.5	68	70	66	66	69	69	70	68	66	67	67	67
2.0	85	86	87	85	87	89	87	88	87	87	85	86
2.5	95	95	96	96	95	97	94	96	96	96	95	94
3.0	98	98	99	98	98	99	98	99	99	99	99	98
3.5	100	99	99	100	100	100	99	100	100	100	100	99
4.0		100	100				100					100

* Determined by sieving
** Uncalibrated values

TABLE 3

Sample- Fine
Size - 10 grams

Size*	Distribution-- percent coarser**											
Ø Units	1	2	3	4	5	6	7	8	9	10	11	12
0.5	2	1	1	2	2	1	1	2	1	1	2	2
1.0	15	10	8	11	12	12	8	10	9	6	10	10
1.5	32	20	17	13	26	24	19	24	24	22	26	24
2.0	53	49	46	50	49	49	47	53	51	45	48	55
2.5	79	77	75	73	76	77	75	76	80	75	75	76
3.0	88	87	86	85	86	89	87	87	90	87	87	87
3.5	95	96	95	93	95	96	95	96	97	95	95	95
4.0	100	100	100	99	100	100	100	100	100	100	100	100

Sample- Intermediate
Size - 10 grams

Size*	Distribution--percent coarser**											
Ø Units	1	2	3	4	5	6	7	8	9	10	11	12
-0.5	0	0	0	1	0	1	1	1	0	0	0	0
0.0	2	2	1	2	1	3	2	2	1	2	2	2
0.5	6	6	6	7	6	8	8	7	6	7	7	6
1.0	31	29	30	31	31	34	31	32	35	31	30	31
1.5	50	50	48	49	50	51	52	51	55	53	55	53
2.0	71	78	73	75	75	75	73	74	76	76	76	75
2.5	90	91	91	92	91	91	90	91	91	91	92	90
3.0	96	97	96	97	96	96	96	97	96	96	97	95
3.5	99	99	99	99	99	99	99	99	99	99	99	100
4.0	100	100	100	100	100	100	100	100	100	100	100	

(continued)

TABLE 3-(continued)

Sample- Coarse
Size - 10 grams

Size*	Distribution--percent coarser**											
Ø Units	1	2	3	4	5	6	7	8	9	10	11	12
-0.5	1	2	1	2	2	1	1	2	1	2	2	1
0.0	5	6	6	7	8	6	5	7	7	7	7	6
0.5	17	20	21	21	23	20	20	24	22	18	21	19
1.0	51	56	56	56	56	53	55	57	52	52	58	52
1.5	69	72	74	73	74	70	70	74	70	70	72	67
2.0	86	88	88	89	91	87	87	90	87	88	88	86
2.5	96	97	96	97	97	96	96	98	97	97	97	96
3.0	99	99	98	99	99	99	99	100	99	99	99	99
3.5	100	100	99	100	100	100	100		100	100	100	100
4.0			100									

* Determined by sieving
** Uncalibrated values

TABLE 4

Sample- Fine
Size - 5 grams

Size Ø Units	Sieve Distribution percent coarser	Average Experimental Distribution-$\bar{X}$* percent coarser	Standard Deviation σ_x
0.5	2	1.5	0.8
1.0	7	9.9	1.8
1.5	20	20.2	3.0
2.0	40	50.3	3.7
2.5	66	76.5	3.1
3.0	84	87.7	1.8
3.5	95	95.3	1.5
4.0	100	99.8	0.4

Sample- Intermediate
Size - 5 grams

Size Ø Units	Sieve Distribution percent coarser	Average Experimental Distribution-$\bar{X}$* percent coarser	Standard Deviation σ_x
-0.5	0.5	0.0	0.0
0.0	2.5	1.7	0.6
0.5	8	6.6	1.3
1.0	22	25.6	2.5
1.5	44	47.6	2.0
2.0	68	73.3	1.4
2.5	86	89.5	1.3
3.0	95	95.3	0.6
3.5	99	98.8	0.4
4.0	100	99.9	0.3

(continued)

TABLE 4-(continued)

Sample- Coarse
Size - 5 grams

Size Ø Units	Sieve Distribution percent coarser	Average Experimental Distribution-$\bar{X}$* percent coarser	Standard Deviation σ_x
-0.5	2	1.8	1.0
0.0	8	5.9	1.2
0.5	22	19.9	1.0
1.0	42	48.9	1.4
1.5	66	67.8	1.4
2.0	85	86.6	1.2
2.5	95	95.4	0.9
3.0	98.8	98.5	0.5
3.5	99.8	99.7	0.5
4.0	100	100.0	0.0

* Averaged over 12 duplicate runs

TABLE 5

Sample- Fine
Size - 10 grams

Size Ø Units	Sieve Distribution percent coarser	Average Experimental Distribution-$\bar{X}$* percent coarser	Standard Deviation σ_x
0.5	2	1.5	0.5
1.0	7	10.1	2.2
1.5	20	22.6	4.7
2.0	40	49.7	2.9
2.5	66	76.2	1.8
3.0	84	87.2	1.3
3.5	95	95.3	0.9
4.0	100	99.9	0.3

Sample- Intermediate
Size - 10 grams

Size Ø Units	Sieve Distribution percent coarser	Average Experimental Distribution-$\bar{X}$* percent coarser	Standard Deviation σ_x
-0.5	0.5	0.3	0.5
0.0	2.5	1.8	0.6
0.5	8	6.7	0.7
1.0	22	31.3	1.6
1.5	44	51.5	2.1
2.0	68	74.8	1.7
2.5	86	90.9	0.6
3.0	95	96.3	0.6
3.5	99	99.1	0.3
4.0	100	100.0	0.0

(continued)

TABLE 5-(continued)

Sample- Coarse
Size - 10 grams

Size Ø Units	Sieve Distribution percent coarser	Average Experimental Distribution-$\bar{X}$* percent coarser	Standard Deviation σ_x
-0.5	2	1.8	0.5
0.0	8	6.4	0.9
0.5	22	20.5	1.9
1.0	42	54.5	2.3
1.5	66	71.3	2.2
2.0	85	87.9	1.4
2.5	95	96.7	0.6
3.0	98.8	99.0	0.4
3.5	99.8	99.9	0.3
4.0	100	100.0	0.0

* Averaged over 12 duplicate runs

DISCUSSION OF RESULTS

As the first step in investigating the characteristics of the sediment analyzer single phi sizes were run, and the resulting fall velocities were compared with the calculated theoretical fall velocities. The experimental results for each phi class were very consistent (table 1). At the level of accuracy of the readings (1 decimal place for most sizes) differences between runs occurred only in the -2.0 phi, -0.5 phi and +2.0 phi classes. The largest standard deviation was observed for the -2.0 phi class (σ_x = 1.1 cm/sec). Two factors probably contributed to this deviation. First, because of the size of the spheres, only three particles were present in each run. Since these particles could range in size from -2.0 phi to -2.5 phi their fall velocities may be expected to differ significantly. Second, these spheres did not settle with a uniform path. Erratic and unexplainable fluctuations in the fall direction occurred during settling which caused collisions with the sides of the settling tube. The deviations for the -0.5 phi and +2.0 phi class are not so easily explained. Perhaps they were due to unassignable operator errors such as in the rotation of the introduction device. Because this device is manual some experience is required in its operation. The main difficulty lies in rotating the cylinder without causing undue vibrations and turbulence. The operation must be performed smoothly but firmly. The procedure adopted was to ro-

tate the cylinder to the halfway position, pause for approximately five seconds until fluctuations of the recorder pen ceased and then complete the rotation. In this manner a smooth distribution curve could be obtained (fig. 4a).

Generally the experimental fall velocities were greater than those calculated theoretically for each sieve opening size. The exact reason for this is unknown, but most likely is caused by settling convection resulting from a relatively dense "cloud" of sedimentary particles falling as a group.

An uncalibrated overlay was constructed from the settling velocities of single phi sizes for use with the multiple phi class distribution. In this study no attempt was made to calibrate the sediment analyzer because to do this hundreds of samples with known fall velocity distributions are required. Instead the main purpose was to determine the consistency or lack of consistency of the apparatus and to determine how it could be improved. To this end the uncalibrated overlay was a sufficient tool.

The 72 runs of the fine, intermediate and coarse distributions were analyzed with the overlay. A survey of the results (tables 2 and 3) and the averages (tables 4 and 5) shows that for the smaller phi sizes the fall time of sediment for any given size class in a multiple size distribution is longer than the corresponding fall time when a single phi class is present. Conversely the coarsest two or three classes in a multiple distribution settle more quickly. These con-

clusions are based on a comparison of the sieve and experimental distributions. The quantitative expression of such deviations is what constitutes a calibration of the apparatus. The method for determining the fall time for each class in a multiple distribution would be to use the recorded curve in the opposite sense to what was done in this study. Known cumulative percents are determined on the curve and the corresponding fall times are read off along the time scale at the bottom of the graph.

The greater fall times for most classes in a multiple distribution can be explained by hindered settling. Consider first a single particle falling with a constant velocity in water. As the particle sinks the water flows up around it. When a large population of grains is present the upward flow around each grain tends to retard the fall of neighbouring grains. Because of this mutual interference the fall velocity of those grains settling in a "cloud" is decreased. For the larger phi sizes in which settling velocity was increased the following explanation is proposed. Because the phi scale of size divisions is essentially logarithmic the fall velocity of sediment particles is distributed logarithmically when plotted against phi size. Therefore, in the coarser sand sizes the fall velocity for successive phi classes increases much more quickly than at the finer end of the scale. When a sample ranging in size from fine to coarse sand is introduced into the top of a sedimentation column the result is that the coarser sizes will

quickly move to the advancing front of the sinking sample and leave the bulk of the sample behind. Then their fall velocities are no longer hindered. This combined with the fact that after the initial introduction of the sediment the fall is momentarily accelerated accounts for the observed increase in settling velocity for the coarsest sizes. Clearly, settling convection and hindered settling vary greatly according to the type of sample.

From Tables 2 and 3 it is apparent that, although the cumulative percentages for the sieve and experimental analyses are different, they generally parallel one another. This suggests that the sorting characteristics for the curves should be nearly identical. Probability plots of the experimental results (not shown) gave similar slopes, showing that this was indeed the case. Figure 7 shows that the maximum deviations between the sieve and experimental analyses occur in the central part of the distribution where the probability cumulative percent scale is compressed.

Analysis of variance was used in this report to study the consistency of the apparatus and the effect of concentration and sample distribution on experimental results. The basic experiment was to run three sample distributions, each at two concentrations, and this was repeated twelve times. The reason for this replication of design was to provide a more reliable estimate of the experimental error, and to decrease the estimate of the variance of designated factors in the

experiment (Ostle, 1956).

The results suggest that oeer the range of sample sizes used (5 and 10 grams) little if any of the variance between runs can be attributed to concentration, except for the 1.0 phi class. No satisfactory explanation can be given to account for this one anomalous result. It is concluded that for samples of 5 to 10 grains no attention is required to sample size in interpreting the curve analyses.

Interaction may be defined as the differential response to one factor in combination with varying levels of a second factor applied simultaneously (Ostle, 1956). The result is that the two factors (sample size and distribution in this study) combine to produce a third effect. Fortuitously interaction was not significant in the results except for two cases. Since interaction is a direct measure of the inconsistency of results between sample sizes and distributions it is concluded that the experiment yielded consistent results from this standpoint. However, the standard deviation as seen in tables 4 and 5 suggest that further study may be required to increase the precision of the apparatus. Once the maximum precision is achieved, accuracy can be increased by calibration of the sediment analyzer.

CONCLUSIONS

The rapid sediment analyzer built at McMaster University will ultimately provide a fast and accurate method of determining the fall velocity distributions for sands. Accuracy can only be accomplished after a large number of sands with known fall velocity distributions have been analyzed.

The experimental data suggests that the apparatus is capable of accurately determining percentiles even in the extreme fine and coarse tails of a distribution. Thus the calculation of statistical parameters which require the 5 and 95 percentiles will provide no special difficulties.

Observations indicate that further study should be undertaken to minimize the degree of operator experience required to operate the introduction device.

BIBLIOGRAPHY

Colby, B.C., and others, (1957a). The development and calibration of the visual-accumulation tube, St. Anthony Falls Hydraulic Laboratory, Minneapolis, Minnesota, Rept. 11, 109 p.

———— (1957b). Some fundamentals of particle size analysis, St. Anthony Falls Hydraulic Laboratory, Minneapolis, Minnesota, Rept. 12, 55 p.

———— (1958). Operators Manual on the Visual-Accumulation tube method for Sedimentation Analysis of Sands, St. Anthony Falls Hydraulic Laboratory, Minneapolis, Minnesota Rept. K, 19 p.

Emery, K.O.,(1938). Rapid Method of Mechanical Analysis of Sands, Jour. Sedimentary Petrology, V.8, pp 105-110.

Jopling, A.V. (1965). Laboratory Study of the Distribution of Grain Sizes in Cross-bedded Deposits, S.E.P.M., Special Publication No. 12, pp. 53-68.

Krembein, W.C. and Pettijohn, F.J. (1938). Manual of Sedimentary Petrography, D. Appleton-Century Company, Inc., New York, 549 p.

Kuenen, Ph.H. (1968). Settling Convection and Grain-size Analysis, Jour. of Sedimentary Petrology V.38, pp. 817-831.

McNown, J.S. and Malaika, J., (1950). Effects of Particle Shape on Settling Velocity of low Reynold's numbers.

Trans. A.G.U., V.31 pp 74-82.

Ostle, Bernard, (1956). Statistics in Research, 2nd ed., The Iowa State College Press, Ames, Iowa, 487 p.

Schlee, John (1966). A modified Woods Hole Rapid Sediment Analyzer, Jour. of Sedimentary Petrology, V.36, pp. 403-413.

Sinions, D.B., Richardson, E.V. and Nordin, C.F., Jr., (1965). Sedimentary Structures generated by flow in alluvial channels, S.E.P.M. Special Publication No. 12, pp. 34-52.

Vanoni, V.A., and others, (1962). Sediment Transportation Mechanics: Introduction and Properties of Sediment, Journal of Hydraulics Division, Proc. of the Am. Soc. of Civil Eng., V.88, pp. 77-107.

Whitney, G.G., (1960). The Woods Hole RApid Analyzer for Sands, Woods Hole Oceanog. Insti., unpublished ms., Reference No. 60-36, 19 p.

Zeigler, J.M. and Gill, Barbara, (1959). Tables and Graphs for the Settling Velocity of Quartz in Water above the range of Stoke's Law. Woods Hole Oceanog. Inst., unpublished ms., Reference No. 59-36, pl3 p.

Zeigler, J.M., Whitney, G.G., Jr. and Hayes, C.R. (1960). Woods Hole Rapid Sediment Analyzer, Jour. of Sedimentary Petrology, V. 30, pp. 490-495.